Journal of Physics B: Atomic, Molecular and Optical Physics

PAPER

Improving the phase sensitivity of an SU (1, 1) interferometer via a nonlinear phase encoding

To cite this article: Osei Seth *et al* 2020 *J. Phys. B: At. Mol. Opt. Phys.* **53** 205503

IOP Publishing Journal of Physics B: Atomic, Molecular and Optical Physics
J. Phys. B: At. Mol. Opt. Phys. **53** (2020) 205503 (6pp) https://doi.org/10.1088/1361-6455/abaaf8

Improving the phase sensitivity of an SU (1, 1) interferometer via a nonlinear phase encoding

Osei Seth[1], Xinfang Li[1], Heng-Na Xiong[2], Junyan Luo[1] and Yixiao Huang[1,3]

[1] School of Science, Zhejiang University of Science and Technology, Hangzhou, Zhejiang, 310023, People's Republic of China
[2] Department of Applied Physics, Zhejiang University of Technology, Hangzhou 310023, People's Republic of China

E-mail: yxhuang@zust.edu.cn

Received 9 March 2020, revised 23 June 2020
Accepted for publication 30 July 2020
Published 11 September 2020

Abstract

We propose a scheme that a dynamically evolving atom-molecule condensate maps onto an SU(1, 1) interferometer, which includes a nonlinear medium (nonlinear phase encoding). We give an analytical result of the phase uncertainty from the error propagation by measuring the particle number at the output and demonstrate the optimal quantum metrology, which is obtained with a time-reversal protocol. We show the phase sensitivity of the nonlinear medium with time-reversal protocol scales as $1/(2.1N^2)$, which overcome the conventional sensitivity limit of $1/N$. Finally, the effect of the poor particle resolution detection on the phase sensitivity is discussed.

Keywords: phase sensitivity, SU(1, 1) interferometer, quantum metrology

(Some figures may appear in colour only in the online journal)

1. Introduction

The field of quantum enhanced metrology, explores the possibility of using quantum techniques to improve measurement precision than purely classical approaches, has been received a lot of attention in recent years [1–11]. Interferometers, characterized by the uncertainty of a single phase measurement $\Delta\phi$, can provide the most precise measurements. The phase sensitivity of an interferometer is fundamentally bounded by the standard quantum limit (SQL) $\Delta\phi \sim 1/\sqrt{N}$ with the classical resources as an input state, where N is the number of particles inside the interferometer [12, 13]. The phase sensitivity of an interferometer can be improved by using quantum resources [14]. There are many theoretical proposals and experimental techniques are developed to improve the sensitivity [15–20]. By using carefully chosen input states such as the Schröinger's cat state (NOON state), SQL is overcome and the phase sensitivity can be enhanced to approach the Heisenberg limit $\Delta\phi \sim 1/N$ [21–28].

However, most of the current atomic and optical interferometers, so called traditional interferometers as SU(2) interferometers, are made of linear devices such as beam splitters and phase shifters. A new configuration that has drawn considerable interest is the SU(1, 1) interferometer, where two nonlinear beam splitters take the place of two linear beam splitters (BSs) in the traditional interferometer [29]. Such a kind of interferometer is described by the SU(1, 1) group, as opposed to SU(2) for BSs. The correlated state is generated under the nonlinear BSs and hence the precision can be enhanced to beat SQL [30–34]. Such a high sensitivity has resulted in a strong theoretical interest in SU(1, 1) interferometry [35, 36] and its experimental realization in various platforms, such as light [37, 38], spinor Bose–Einstein condensates (BECs) [39–41], and light-atom hybrids [42].

Though the BSs are nonlinear in the SU(1, 1) interferometer, all of the works are focused on the linear phase encoding,

[3] Author to whom any correspondence should be addressed.

and hence the sensitivity of the phase ϕ is limited at the order of $1/N$. Recent work showed that measurement uncertainty of the order $1/N^k$ is possible by using a more general parameter estimation theory, where k is the number of parameter-sensitive terms [43–45]. This formal result demonstrated that the conventional limit is, in fact, the case with $k = 1$ and $k = 2$ may be able to achieve up to $\Delta\phi \sim 1/N^2$ when considering the measurements of atom–atom interactions with two-body collisions (nonlinear phase encoding) [45].

In this paper, we propose a scheme to implement an SU(1, 1) interferometer with nonlinear phase encoding via stimulated dissociation of a molecular BEC, and study phase sensitivity of the phase. The scheme includes two pulses of atom-molecule coupling which are separated by a phase-acquisition period, similar to the Ramsey procedure in [46, 47] but starting from a molecular BEC instead of an atomic one. In the limit where the dissociation does not deplete the molecular BEC, the state will be an SU(1, 1) squeezed state. The nonlinear phase is encoded by tuning Feshbach-resonance coupling and switching the photodissociation lasers for the optical resonant Raman coupling. We give an analytical result of phase uncertainty from the error propagation by measuring the atomic number at the output of the interferometer. We show the optimal phase uncertainty attains it maximum with echo protocol [48–56] which perfectly time reverse the first entangling unitary and then project onto the initial state. We find the optimal phase uncertainty with time reverse scales as $1/(2.1N_{\rm a}^2)$, overcoming the conventional limit of $1/N_{\rm a}$, here $N_{\rm a}$ denotes the particle number insider the interferometer. Finally, we discuss the effect of the detection noise on the phase sensitivity and show the phase sensitivity becomes robust to the noise by increasing the gain of the second beam splitter.

This paper is organized as follows. In section 2, we first briefly introduce atom-molecule BECs and map the dynamically evolving atom-molecule condensate onto the SU(1, 1) interferometer. In section 3, we show the phase sensitivity of the SU(1, 1) interferometer. In section 4, we study the effect of the detection noise on the phase sensitivity. Finally, our conclusions are given in section 5.

2. SU(1, 1) interferometry with atom–molecule condensate

We consider the atom–molecule condensate, where the particles can populate three modes: two atomic modes (1 and 2) and one molecular mode (m). Assuming the spatial wave functions for the modes are fixed and then we associate each mode with an annihilation operator $\hat{a}_i$ of a particle in mode $i(= 1, 2, \mathrm{m})$. The interacting atoms and molecules are coupled by means of either a Feshbach resonance or a resonant Raman transition. Within the three-mode approximation, the second quantized Hamiltonian reads [57–61]

$$\hat{H} = \delta\hat{a}_{\rm m}^\dagger\hat{a}_{\rm m} + \sum_{i,j}\chi_{ij}\hat{a}_i^\dagger\hat{a}_j^\dagger\hat{a}_i\hat{a}_j + g\left(\hat{a}_1^\dagger\hat{a}_2^\dagger\hat{a}_{\rm m} + \hat{a}_{\rm m}^\dagger\hat{a}_1\hat{a}_2\right), \quad (1)$$

where the detuning δ denotes the energy difference between the atomic and molecular levels which can be tuned by an external field, g is the strength of atom-molecule coupling, and χ_{ij} is the s-wave collisional strength between modes i and j. The total number of the system and the difference between the two atomic species are given by $\hat{N} = \hat{a}_1^\dagger\hat{a}_1 + \hat{a}_2^\dagger\hat{a}_2 + 2\hat{a}_{\rm m}^\dagger\hat{a}_{\rm m}$ and $\hat{D} = \hat{a}_1^\dagger\hat{a}_1 - \hat{a}_2^\dagger\hat{a}_2$. Here we note these two quantities obvious constants of motion from Hamiltonian (1). Neglected the constant terms proportional to $\hat{D}$ and $\hat{N}$, the above Hamiltonian reduces to [58]

$$\hat{H} = \frac{\gamma}{\sqrt{2N}}\left(\hat{a}_1^\dagger\hat{a}_2^\dagger\hat{a}_{\rm m} + \hat{a}_{\rm m}^\dagger\hat{a}_1\hat{a}_2\right) + \frac{\Gamma}{4N}\left(\hat{a}_1^\dagger\hat{a}_1 + \hat{a}_2^\dagger\hat{a}_2\right)^2 - \frac{\Delta}{2}\left(\hat{a}_1^\dagger\hat{a}_1 + \hat{a}_2^\dagger\hat{a}_2\right), \quad (2)$$

where $\Gamma = N[\chi_{11} + \chi_{22} + \chi_{\rm mm} + 2(\chi_{12} - \chi_{\rm m1} - \chi_{\rm m2})]$, $\Delta = [\delta - (D-1)\chi_{11} + (D+1)\chi_{22} + (N-1)\chi_{\rm mm} - (N-D)\chi_{\rm m1} - (N+D)\chi_{\rm m2}]$, and $\gamma = g\sqrt{2N}$ being the rescaled atom–molecule coupling strength.

In this paper, we consider the short-time dynamics of molecular dissociation which enables the molecular condensate remains large and is never significantly depleted by the conversion of a small number of molecules into atoms, i.e. $N_{\rm m} = \hat{a}_{\rm m}^\dagger\hat{a}_{\rm m} \approx N/2$. Under this condition, the molecular creation and annihilation operators $\hat{a}_{\rm m}^\dagger$ and $\hat{a}_{\rm m}$ can be replaced by a c number $\sqrt{N_{\rm m}}$ and the Hamiltonian with neglecting the constant terms can be remarkably simplified as [57]

$$H = \lambda\hat{K}_z + \mu\hat{K}_x + \chi\hat{K}_z^2, \quad (3)$$

where the parameters $\lambda = -\Delta$, $\mu = \gamma$, and $\chi = \frac{\Gamma}{N}$. The operators $\hat{K}_x = (\hat{a}_1^\dagger\hat{a}_2^\dagger + \hat{a}_1\hat{a}_2)/2$, $\hat{K}_y = (\hat{a}_1^\dagger\hat{a}_2^\dagger - \hat{a}_1\hat{a}_2)/(2i)$, and $\hat{K}_z = (\hat{a}_1^\dagger\hat{a}_1 + \hat{a}_2^\dagger\hat{a}_2 + 1)/2$ belong to the SU(1, 1) Lie algebra and satisfy the canonical commutation relations $[\hat{K}_x, \hat{K}_y] = -i\hat{K}_z$, $[\hat{K}_x, \hat{K}_z] = -i\hat{K}_y$, and $[\hat{K}_y, \hat{K}_z] = i\hat{K}_x$. The mutual eigenstates of the Casimir operator $\hat{K}^2$ and $\hat{K}_z$ form the basis set $(\hat{K}_z^2 - \hat{K}_x^2 - \hat{K}_y^2)|n,k\rangle = k(k-1)|n,k\rangle$ and $\hat{K}_z|n,k\rangle = (n+k)|n,k\rangle$ with $n = 0, 1, 2, \ldots$, and k is called the Bargmann index. Considering two modes case, we have $k = 1/2$.

Now we map the dynamically evolving atom–molecule condensate onto the SU(1, 1) interferometer. The structure of the interferometer consists of five steps: (I) probe state preparation (we consider that all of the particles are condensate at the molecular mode), (II) a first dynamics of molecular dissociation, (III) phase encoding, (IV) a second dynamics of molecular dissociation, and (V) the particle number in the atomic modes are measured.

3. Measurement precision

Starting from the atom vacuum state $|0, 1/2\rangle$ which corresponds to the molecular BEC. Then the second step of the dissociation is a small fraction of the molecular BEC into atoms by setting $\mu \gg \lambda, \chi$, the atomic coherent state is obtained and given by

$$|\psi_1\rangle = \mathrm{e}^{-i\hat{K}_x\tau_1}|0, 1/2\rangle \quad (4)$$

with $\tau_1 = \mu t_1$. The parameter condition $\mu \gg \lambda, \chi$ can be

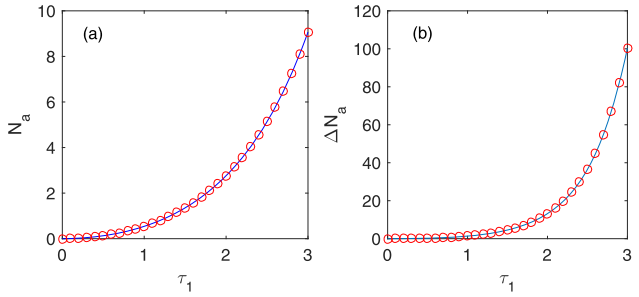

Figure 1. (a) Particle number of atoms and (b) the variance as a function of τ_1. Circles and line correspond to numerical results of Hamiltonian (1) and analytical results of equations (5) and (6), respectively. The total particle number for numerical calculation is chosen as $N = 5000$, which is same for the following calculations.

easily attained in the current experiment by using the magnetic control of the atom–molecule detuning for Feshbach-resonance coupling and switching the photodissociation laser for the optical resonant Raman coupling. The atomic number inside the interferometer N_a, defined as $N_a = 2\langle\psi_1|\hat{K}_z|\psi_1\rangle - 1$, and the correspondence variance ΔN_a^2 are given by

$$N_a = 2\,\sinh^2\frac{\tau_1}{2}, \tag{5}$$

$$\Delta N_a^2 = N_a(N_a+2). \tag{6}$$

The coherent atomic population and the variance dynamics starting from the vacuum as a function of τ_1 are plotted in figure 1. The numerical results obtained from Hamiltonian equation (1) coincide well with the analytical results. It is therefore clear that the evolution state of the system will remain an SU(1, 1) coherent state when the molecular mode is macroscopically populated.

Next, the coupling μ is turned off and the atomic interaction phase is allowed to evolve for a hold time t_h. In the limit of $\chi \gg \lambda$, the state at the end of the hold time is $|\psi_\theta\rangle$ which is defined as $|\psi_\theta\rangle = e^{-i\chi\hat{K}_z^2 t_h}|\psi_1\rangle$. Such a unitary transformation encodes the phase $\theta = \chi t_h$. The phase may be determined by a second strong coupling pulse of duration which is described by $e^{-i\hat{K}_x\tau_2}$ and the final state is given by $|\psi_f\rangle = e^{-i\hat{K}_x\tau_2}|\psi_\theta\rangle$. Hence the structure of the scheme combined boost-phase-boost sequence $e^{-i\hat{K}_x\tau_2}e^{-i\theta\hat{K}_z^2}e^{-i\hat{K}_x\tau_1}$. The phase shift θ is estimated by measuring the number of particles $\mathcal{N}_{out}$, with $\mathcal{N}_{out} \equiv 2\langle\psi_f|\hat{K}_z|\psi_f\rangle - 1$, in the atomic modes at the end of the interferometric sequence. We calculate the phase uncertainty as

$$\Delta\theta = \frac{\Delta\mathcal{N}_{out}}{|d\mathcal{N}_{out}/d\theta|}. \tag{7}$$

At the end of the interferometer, $\mathcal{N}_{out}$ and the variance $\Delta\mathcal{N}_{out}$ are given by

$$\mathcal{N}_{out} = 2\,\sinh\,\tau_2\,\sinh\,\tau_1\frac{\cos\,2\theta\,(1+\cosh^2\tau_1)-\sinh^2\tau_1}{(1+\cosh^2\tau_1-\sinh^2\tau_1\,\cos\,2\theta)^2}+\cosh\,\tau_2\,\cosh\,\tau_1-1, \tag{8}$$

$$\begin{aligned}\Delta\mathcal{N}_{out} = \Bigg\{&\sinh^2\tau_2\left[\frac{2\,\sinh^2\tau_1\left[(1+3\,\cosh^2\tau_1)\cos\,6\theta-3\,\sinh^2\tau_1\,\cos\,2\theta\right]}{(1+\cosh^2\tau_1-\sinh^2\tau_1\,\cos\,4\theta)^3}-\frac{(4\,\sinh^3\tau_1-\cos\,2\theta\,(5\,\sinh\,\tau_1+\sinh\,3\tau_1))^2}{4(1+\cosh^2\tau_1-\sinh^2\tau_1\,\cos\,2\theta)^4}\right]\\&-\sinh\,2\tau_2\frac{(27\,\sinh\,2\tau_1+4\,\sinh\,4\tau_1-6\,\sinh\,6\tau_1)\cos\,2\theta+4\,\cosh\,\tau_1\,\sinh^3\tau_1\,[3\,\cosh\,2\tau_1-15+\cos\,4\theta\,(11+\cosh\,2\tau_1)]}{8(1+\cosh^2\tau_1-\cos\,2\theta\,\sinh^2\tau_1)^3}\\&+\sinh^2\tau_2\,\cosh^2\tau_1+\cosh^2\tau_2\,\sinh^2\tau_1\Bigg\}^{1/2}.\end{aligned} \tag{9}$$

As shown in figures 2(a) and (b), the particle number and the variance in the atomic modes are plotted as a function of phase shift θ. The numerical results of Hamiltonian equation (1) coincide well with the analytical ones in equations (8) and (9). The rescaled phase uncertainties $\Delta\tilde{\theta} = 1/\Delta\theta$ are also plotted in figure 2 for different τ_2/τ_1 with $\tau_1 = 2$. It can be clearly seen $\Delta\tilde{\theta}$ exhibit different behaviors by varying τ_2/τ_1. $\Delta\tilde{\theta}$ attains its maximal value at special θ for different τ_2/τ_1. When $\tau_2/\tau_1 = -1$, corresponds to the time-reversal scheme (echo protocol), $\Delta\tilde{\theta}$ attains its maximal value at $\theta = 0$. In the previous studies, most of the works were focused on the echo case, here we discuss the effect of τ_2 on the phase uncertainty.

As shown in figure 3(a), the optimal phase uncertainty $\Delta\tilde{\theta}_{opt}$, defined as $\Delta\tilde{\theta}_{opt} = \max_\theta(\Delta\tilde{\theta})$, is plotted as a function of τ_2/τ_1. The phase sensitivity in the regime $\tau_2/\tau_1 < -1$ is much better than that in the regime $\tau_2/\tau_1 > 1$. When $|\tau_2|$ is large enough, $\Delta\tilde{\theta}_{opt}$ is nearly independent on the τ_2. The optimal phase sensitivity is obtained when $\tau_2/\tau_1 = -1$, which means the optimal interferometer configuration is reached for the time-reversal protocol. Such a protocol, perfectly time reverse the first entangling unitary and then project onto the initial state, with linear phase encoding has been shown to saturate the quantum Cramér–Rao bound for arbitrary pure states [54], which indicates the time-reversal protocol to be the optimal quantum metrology. Here, the interferometer with nonlinear phase encoding has the same property. The optimal phase θ_{opt} is also plotted in figure 3(b), it is shown θ_{opt} is nearly independent on τ_2 when it is large enough, which is similar to the behavior of $\Delta\tilde{\theta}_{opt}$.

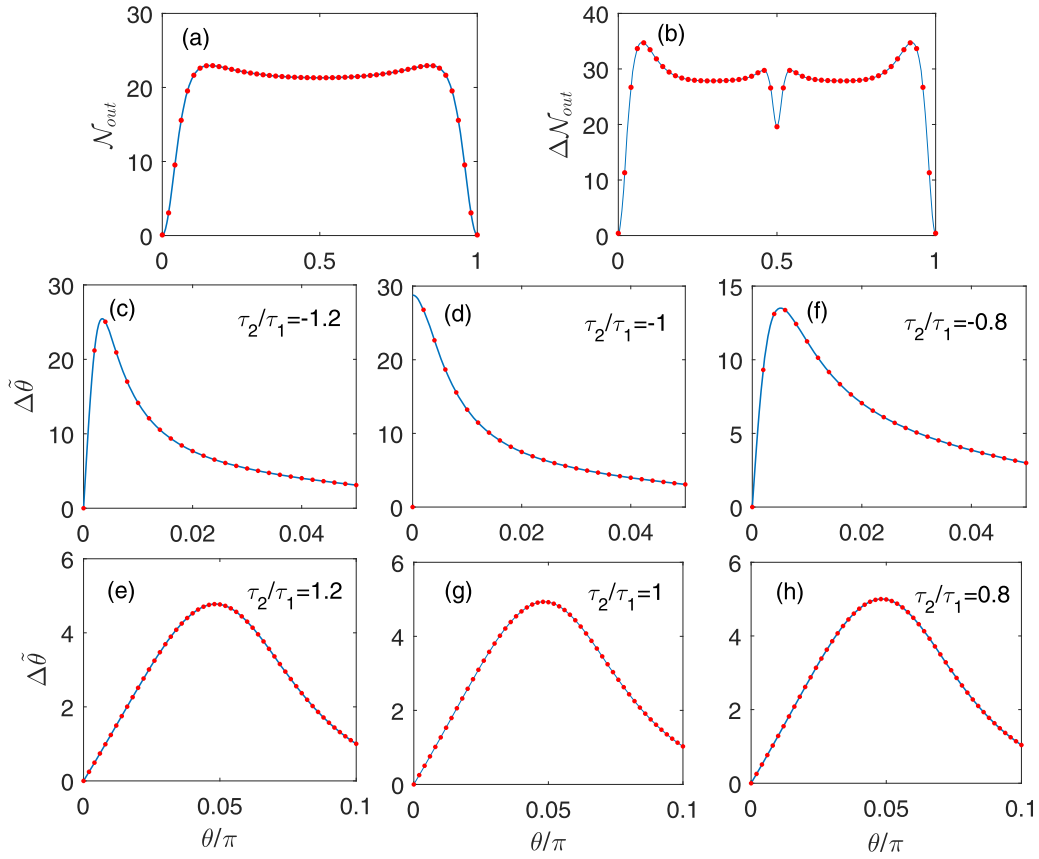

Figure 2. (a) $\mathcal{N}_{\rm out}$ and (b) $(\Delta\mathcal{N})^2_{\rm out}$ as a function of θ with $\tau_2/\tau_1 = -1.2$. (c)–(h) $\Delta\tilde{\theta}$ as a function of phase shift θ for different ratio τ_2/τ_1 with $\tau_1 = 2$. The symbols and solid lines correspond to numerical results of Hamiltonian (1) and analytical results of equations (7)–(9), respectively.

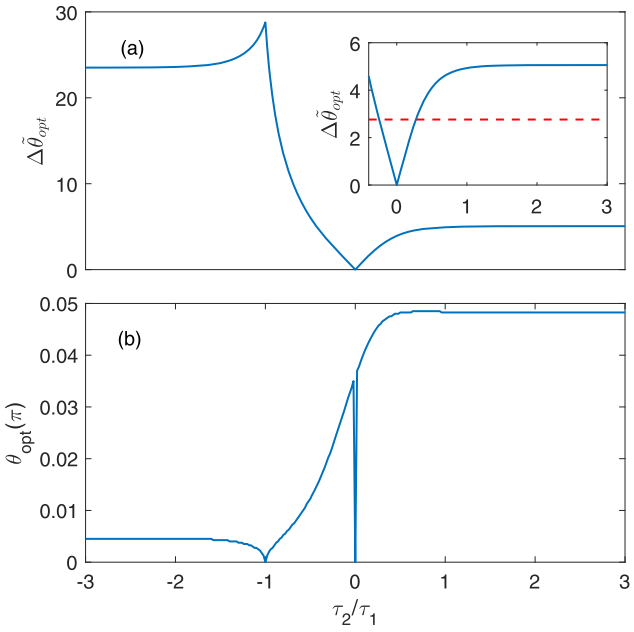

Figure 3. (a) $\Delta\tilde{\theta}_{\rm opt}$ and (b) the optimal angle $\theta_{\rm opt}$ as a function of τ_2/τ_1 with $\tau_1 = 2$. The inset shows the parameter τ_2/τ_1 varies from -0.4 to 3 and the red dashed line denote the fundamental limit for the linear phase encoding, i.e. $\sim 1/N_{\rm a}$.

Though phase sensitivity can be improved through the nonlinear phase encoding, the collisional interaction may result in the loss of atom–molecule phase coherence on a time scale $\tau_{\rm pd} = 1/(2N_{\rm a}\chi)$ [57]. As shown in figure 3(b), when $\tau_2/\tau_1 < 0$, $\theta_{\rm opt} < \chi\tau_{\rm pd} = \frac{1}{5.52}$. While $\theta_{\rm opt} > \chi\tau_{\rm pd}$ as τ_2/τ_1 increases.

For the SU(1, 1) interferometry with linear phase, i.e. $e^{-i\hat{K}_z\theta}$, the fundamental limit of the phase sensitivity is $N_{\rm a}(N_{\rm a}+2)$ which indicates $\Delta\theta \sim 1/N_{\rm a}$. The inset of figure 3(a) shows the optimal phase uncertainty $\Delta\tilde{\theta}_{\rm opt}$ with nonlinear phase can easily beat the fundamental limit by tuning τ_2. In figure 4, we show the scaling of $\Delta\tilde{\theta}_{\rm opt}$ versus $N_{\rm a}$ at $\tau_2/\tau_1 = -1$. A fit of the data gives the optimal sensitivity as

$$\Delta\tilde{\theta}_{\rm opt} = 2.1N_{\rm a}^2 + 4.5N_{\rm a} + 0.4. \tag{10}$$

When $N_{\rm a}$ is large, $\Delta\tilde{\theta}_{\rm opt} \sim 2.1N_{\rm a}^2$. Therefore, the sensitivity of parameter estimation can be greatly improved with a nonlinear phase encoding. In fact, the quantum fisher information for the state $|\psi_1\rangle$ is

$$F_{\rm Q} = 4(\Delta\hat{K}_z^2)^2 = 5[N_{\rm a}(N_{\rm a}+2)]^2 + 4N_{\rm a}(N_{\rm a}+2). \tag{11}$$

When $N_{\rm a} \gg 1$, we have $F_{\rm Q} \sim 5N_{\rm a}^4$. Thus the quantum Cramé r–Rao bound for such a nonlinear phase encoding is $\Delta\tilde{\theta}_{\rm opt} \leqslant \sqrt{5}N_{\rm a}^2$.

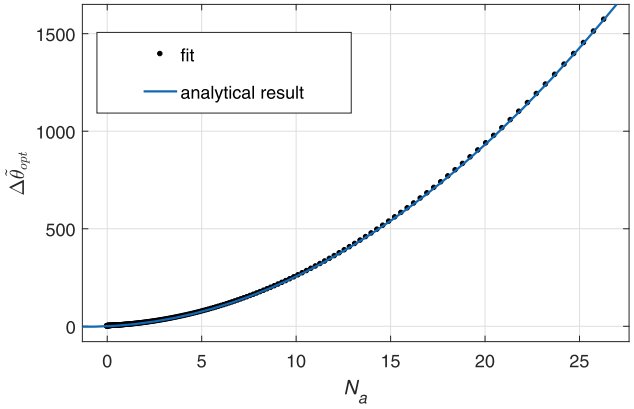

Figure 4. Scaling of $\Delta\tilde{\theta}_{\rm opt}$ as a function of $N_{\rm a}$. Solid line is the numerical result, while the dots are polynomial fits.

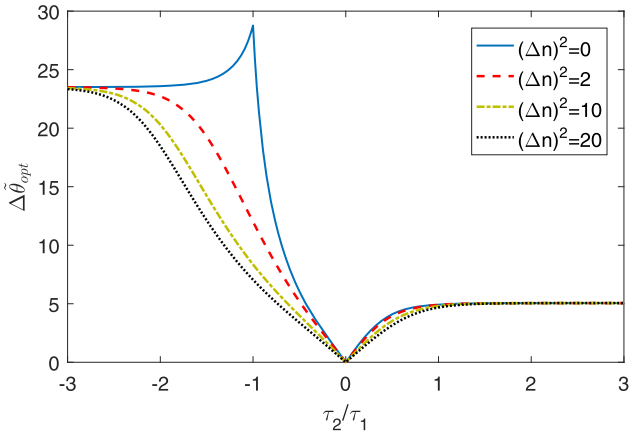

Figure 5. $\Delta\tilde{\theta}_{\rm opt}$ as a function of τ_2/τ_1 with $\tau_1 = 2$ for different detection noise $(\Delta n)^2$.

4. Detection noise

The amount of measured sensitivity is limited by several factors in the practice. The largest influence is the particle-independent detection noise which makes n and $n + \Delta n$ particles indistinguishable and arises mostly from the photon shot noise of the probe light. Quantum-enhanced measurements typically require single-particle resolution ($\Delta n \sim 1$). Here, we consider an imperfect detection resolution as a type of Gaussian noise with variance $(\Delta n)^2$, which corresponds to an uncertainty Δn in the particle number measured at the end of the interferometer. Such a technical noise increases the quantum noise on the measurement signal, and the phase sensitivity is modified as [48]

$$\Delta\theta_{\rm opt} = \frac{\sqrt{\Delta\mathcal{N}_{\rm out}^2 + (\Delta n)^2}}{|d\mathcal{N}_{\rm out}/d\theta|}. \tag{12}$$

In general, the presence of the noise would also modify the optimal operating point. In figure 5, $\Delta\tilde{\theta}_{\rm opt}$ is plotted as a function of τ_2/τ_1 with different noise $(\Delta n)^2$. It is clearly shown the detection noise decreases the phase sensitivity in the regime $\tau_2/\tau_1 < 1$. In particular, the detection noise has a great influence on the sensitivity at $\tau_2/\tau_1 = -1$. It means the echo protocol scheme is not robust to detection noise. Whereas, in the regime $\tau_2 > \tau_1$, the sensitivity $\Delta\tilde{\theta}_{\rm opt}$ is nearly independent on the noise. From figure 5, we can also find $\Delta\tilde{\theta}_{\rm opt}$ to be robust to the noise by increasing $|\tau_2|$ in a negative regime of τ_2/τ_1. Hence, we can increase the value of τ_2 to reduce the effect of the noise on the phase sensitivity.

Before conclusion, we estimate some parameters under current experimental conditions. In the zero-range single-channel scattering approximation, the molecule–molecule and atom–molecule s-wave scattering lengths are approximated as $a_{\rm m} \approx 0.6a_{\rm a}$, $a_{\rm am} \approx 1.2a_{\rm a}$ with $a_{\rm a}$ being the bohr radius [62, 63]. Assuming a molecular BEC of 10^4 (with 0.2% dissociation) are trapped in a 100 Hz spherical trap, the dephasing of the molecular field takes place on a time scale on the order of 10 ms. If we consider the frequency of the trap with 10^4 Hz, the atom–molecule Feshbach conversion frequency becomes to 1 MHz and the dephasing time will be also much larger. Then the dephasing can be neglected during the phase encoding.

5. Conclusion

In summary, we have proposed a scheme to realize an SU(1, 1) interferometer with nonlinear phase encoding. We mapped a short time dynamically evolving atom–molecule condensate onto the SU(1, 1) interferometer. We discussed the phase sensitivity of the interferometer with different τ_2/τ_1 and show the sensitivity in the regime $\tau_2/\tau_1 < -1$ is much better than that in the regime $\tau_2/\tau_1 > 1$. In particular, we found optimal phase sensitivity is obtained at $\tau_2 = -\tau_1$, which means the echo protocol is optimal for the metrology. We also discussed the optimal sensitivity $\Delta\tilde{\theta}_{\rm opt}$ versus the population of atoms inside the interferometer and showed the scaling of $\Delta\tilde{\theta}_{\rm opt} \sim 2.1N_{\rm a}^2$ which is overcome the conventional limit. The effect of the detection noise is also discussed on the phase sensitivity. Our results may suggest new implications for quantum metrology.

Acknowledgments

This work was supported by the Natural Science Foundation of China (No. 11605157 and No. 11774311).

ORCID iDs

Yixiao Huang https://orcid.org/0000-0003-4628-5104

References

[1] Helstrom C W 1976 *Quantum Detection and Estimation Theory* (New York: Academic)
[2] Holevo A S 2011 *Probabilistic and Statistical Aspects of Quantum Theory* (Berlin: Springer)
[3] Caves C M 1981 *Phys. Rev.* D **23** 1693
[4] Braunstein S L and Caves C M 1994 *Phys. Rev. Lett.* **72** 3439
[5] Braunstein S L, Caves C M and Milburn G J 1996 *Ann. Phys., NY* **247** 135
[6] Lee H, Kok P and Dowling J P 2002 *J. Mod. Opt.* **49** 2325
[7] Giovannetti V, Lloyd S and Maccone L 2006 *Phys. Rev. Lett.* **96** 010401
[8] Zwierz M, Pérez-Delgado C A and Kok P 2010 *Phys. Rev. Lett.* **105** 180402

[9] Giovannetti V, Lloyd S and Maccone L 2004 *Science* **306** 1330
[10] Giovannetti V, Lloyd S and Maccone L 2011 *Nat. Photon.* **5** 222
[11] Ou Z Y 2012 *Phys. Rev.* A **85** 023815
[12] Jarzyna M and Demkowicz-Dobrzański R 2012 *Phys. Rev.* A **85** 011801(R)
[13] Pezzè L and Smerzi A 2009 *Phys. Rev. Lett.* **102** 100401
[14] Wineland D J, Bollinger J J, Itano W M, Moore F L and Heinzen D J 1992 *Phys. Rev.* A **46** R6797
[15] Zhang J-D, Zhang Z-J, Cen L-Z, Hu J-Y and Zhao Y 2019 *Phys. Rev.* A **99** 022106
[16] Spagnolo N, Vitelli C, Lucivero V G, Giovannetti V, Maccone L and Sciarrino F 2012 *Phys. Rev. Lett.* **108** 233602
[17] Zhang J-D, Zhang Z-J, Cen L-Z, Hu J-Y and Zhao Y 2020 arXiv:2001.00160
[18] Tóth G and Apellaniz I 2014 *J. Phys.* A **47** 424006
[19] Pezzé L and Smerzi A 2014 *Atom Interferometry* (*Proceedings of the International School of Physics "Enrico Fermi"* vol 188) (Amsterdam: IOS Press)
[20] Dobrzanski R D, Jarzyna M and Kolodyn J 2015 *Prog. Optics* **60** 345–435
[21] Schnabel R, Mavalvala N, McClelland D E and Lam P K 2010 *Nat. Commun.* **1** 121
[22] Grote H, Danzmann K, Dooley K L, Schnabel R, Slutsky J and Vahlbruch H 2013 *Phys. Rev. Lett.* **110** 181101
[23] Bollinger J J, Itano W M, Wineland D J and Heinzen D J 1996 *Phys. Rev.* A **54** R4649
[24] Huelga S F, Macchiavello C, Pellizzari T, Ekert A K, Plenio M B and Cirac J I 1997 *Phys. Rev. Lett.* **79** 3865
[25] Gerry C C and Campos R A 2003 *Phys. Rev.* A **68** 025602
[26] Campos R A, Gerry C C and Benmoussa A 2003 *Phys. Rev.* A **68** 023810
[27] Pezzè L and Smerzi A 2007 *Europhys. Lett.* **78** 30004
[28] Berry D W, Higgins B L, Bartlett S D, Mitchell M W, Pryde G J and Wiseman H M 2009 *Phys. Rev.A* **80** 052114
[29] Yurke B, McCall S L and Klauder J R 1986 *Phys. Rev.* A **33** 4033
[30] Leonhardt U 1994 Quantum statistics of a two-mode SU(1, 1) interferometer *Phys. Rev.* A **49** 1231
[31] Vourdas A 1990 *Phys. Rev.* A **41** 1653
[32] Sanders B C, Milburn G J and Zhang Z 1997 *J. Mod. Opt.* **44** 1309
[33] Liu S, Lou Y, Xin J and Jing J 2018 *Phys. Rev. Appl.* **10** 064046
[34] Wang H, Marino A M and Jing J 2015 *Appl. Phys. Lett.* **107** 121106
[35] Chen Z-D, Yuan C-H, Ma H-M, Li D, Chen L Q, Ou Z Y and Zhang W 2016 *Opt. Express* **24** 17766
[36] Xin J, Wang H and Jing J 2016 *Appl. Phys. Lett.* **109** 051107
[37] Jing J, Liu C, Zhou Z, Ou Z Y and Zhang W 2011 *Appl. Phys. Lett.* **99** 011110
[38] Hudelist F, Kong J, Liu C, Jing J, Ou Z Y and Zhang W 2014 *Nat. Commun.* **5** 3049
[39] Gross C, Zibold T, Nicklas E, Estève J and Oberthaler M K 2010 *Nature* **464** 1165
[40] Peise J, Lücke B, Pezzé L, Deuretzbacher F, Ertmer W, Arlt J, Smerzi A, Santos L and Klempt C 2015 *Nat. Commun.* **6** 6811
[41] Linnemann D, Strobel H, Muessel W, Schulz J, Lewis-Swan R J, Kheruntsyan K V and Oberthaler M K 2016 *Phys. Rev. Lett.* **117** 013001
[42] Chen B, Qiu C, Chen S, Guo J, Chen L Q, Ou Z Y and Zhang W 2015 *Phys. Rev. Lett.* **115** 043602
[43] Luis A 2004 *Phys. Lett.* A **329** 8–13
[44] Boixo S, Flammia S T, Caves C M and Geremia J M 2007 *Phys. Rev. Lett.* **98** 090401
[45] Choi S and Sundaram B 2008 *Phys. Rev.* A **77** 053613
[46] Donley E A, Claussen N R, Thompson S T and Wieman C E 2002 *Nature* **417** 529
[47] Kokkelmans S J J M F and Holland M J 2002 *Phys. Rev. Lett.* **89** 180401
[48] Davis E, Bentsen G and Schleier-Smith M 2016 *Phys. Rev. Lett.* **116** 053601
[49] Toscano F, Dalvit D A R, Davidovich L and Zurek W H 2006 *Phys. Rev.* A **73** 023803
[50] Goldstein G, Cappellaro P, Maze J R, Hodges J S, Jiang L, Sørensen A S and Lukin M D 2011 *Phys. Rev. Lett.* **106** 140502
[51] Marino A M, Corzo Trejo N V and Lett P D 2012 *Phys. Rev.* A **86** 023844
[52] Ma H, Li D, Yuan C-H, Chen L Q, Ou Z Y and Zhang W 2015 *Phys. Rev.* A **92** 023847
[53] Gabbrielli M, Pezzè L and Smerzi A 2015 *Phys. Rev. Lett.* **115** 163002
[54] Macrì T, Smerzi A and Pezzè L 2016 *Phys. Rev.* A **94** 010102
[55] Manceau M, Khalili F and Chekhova M 2017 *New J. Phys.* **19** 013014
[56] Szigeti S S, Lewis-Swan R J and Haine S A 2017 *Phys. Rev. Lett.* **118** 150401
[57] Tikhonenkov I and Vardi A 2009 *Phys. Rev.* A **80** 051604(R)
[58] Zhou L, Zhang W, Ling H Y, Jiang L and Pu H 2007 *Phys. Rev.* A **75** 043603
[59] Santos G, Tonel A P, Foerster A and Links J 2006 *Phys. Rev.* A **73** 023609
[60] Jing L, Ye D-F, Ma C, Fu L-B and Liu J 2009 *Phys. Rev.* A **79** 025602
[61] Cui B, Wang L C and Yi X X 2012 *Phys. Rev.* A **85** 013618
[62] Petrov D S, Salomon C and Shlyapnikov G V 2004 *Phys. Rev. Lett.* **93** 090404
[63] Jensen L M, Makela H and Pethick C J 2007 *Phys. Rev.* A **75** 033606